Supplementary information

Bimodality of incipient plastic strength in face-centered cubic high-entropy alloys

Yakai Zhao[1], Jeong-Min Park[2], Jae-il Jang[2,*], Upadrasta Ramamurty[1,*]

[1]School of Mechanical and Aerospace Engineering, Nanyang Technological University, Singapore 639798

[2]Division of Materials Science and Engineering, Hanyang University, Seoul 04763, Republic of Korea

* Co-corresponding authors: uram@ntu.edu.sg (U. Ramamurty), jijang@hanyang.ac.kr (J.-i. Jang)

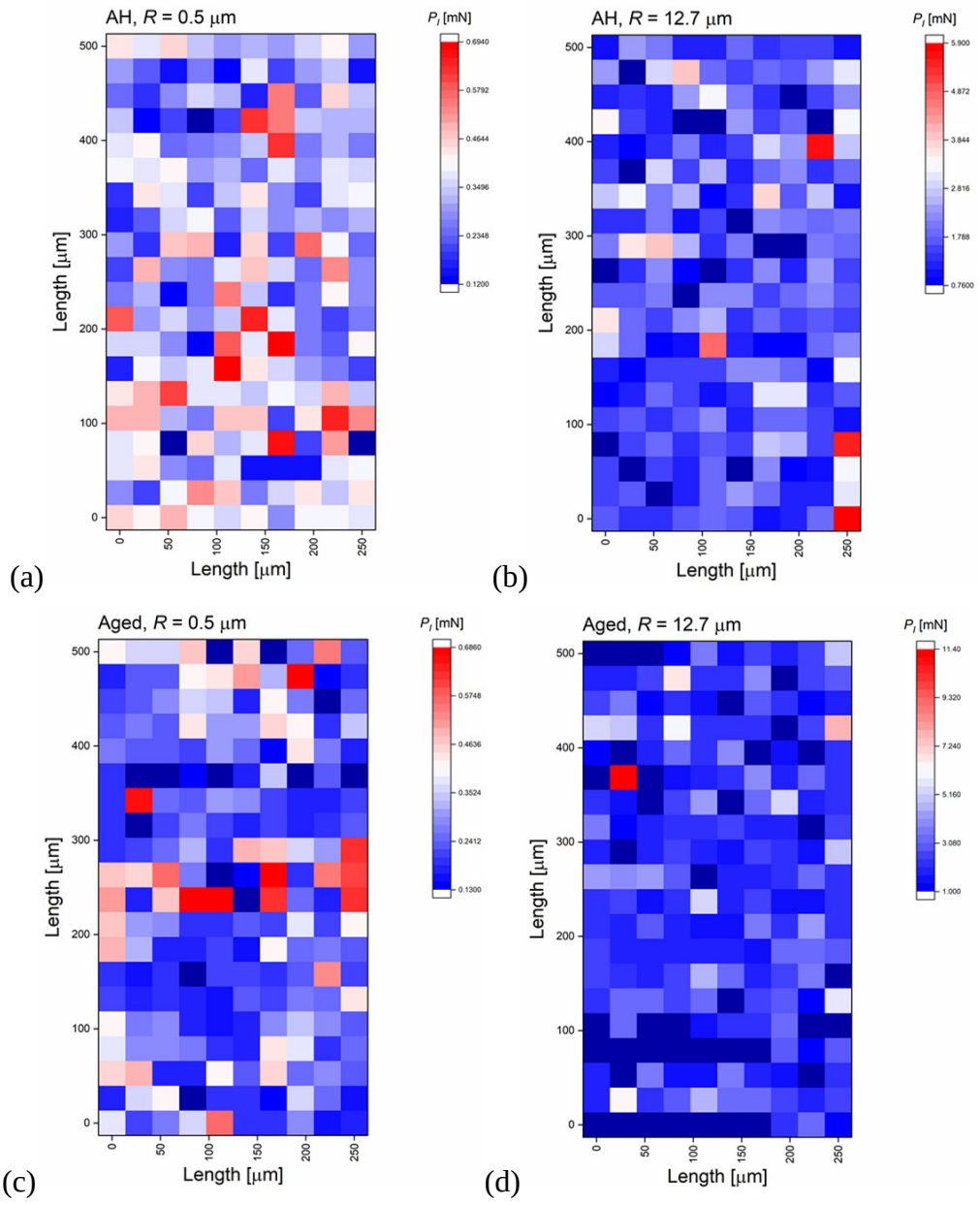

Figure S1 Maps of the first pop-in load, P_I, obtained from AH [(a) and (b)] and Aged CoCrFeMnNi samples [(c) and (d)]. (a) and (c) are for R_i = 0.5 μm, and (b) and (d) are for R_i = 12.7 μm. The interspacing between indents is 25 μm, and the average grain size of both sample are ~ 50 μm. In the maps, there is no significant grain orientation effect on the P_I and hence the possible orientation effect could be neglected in this study.

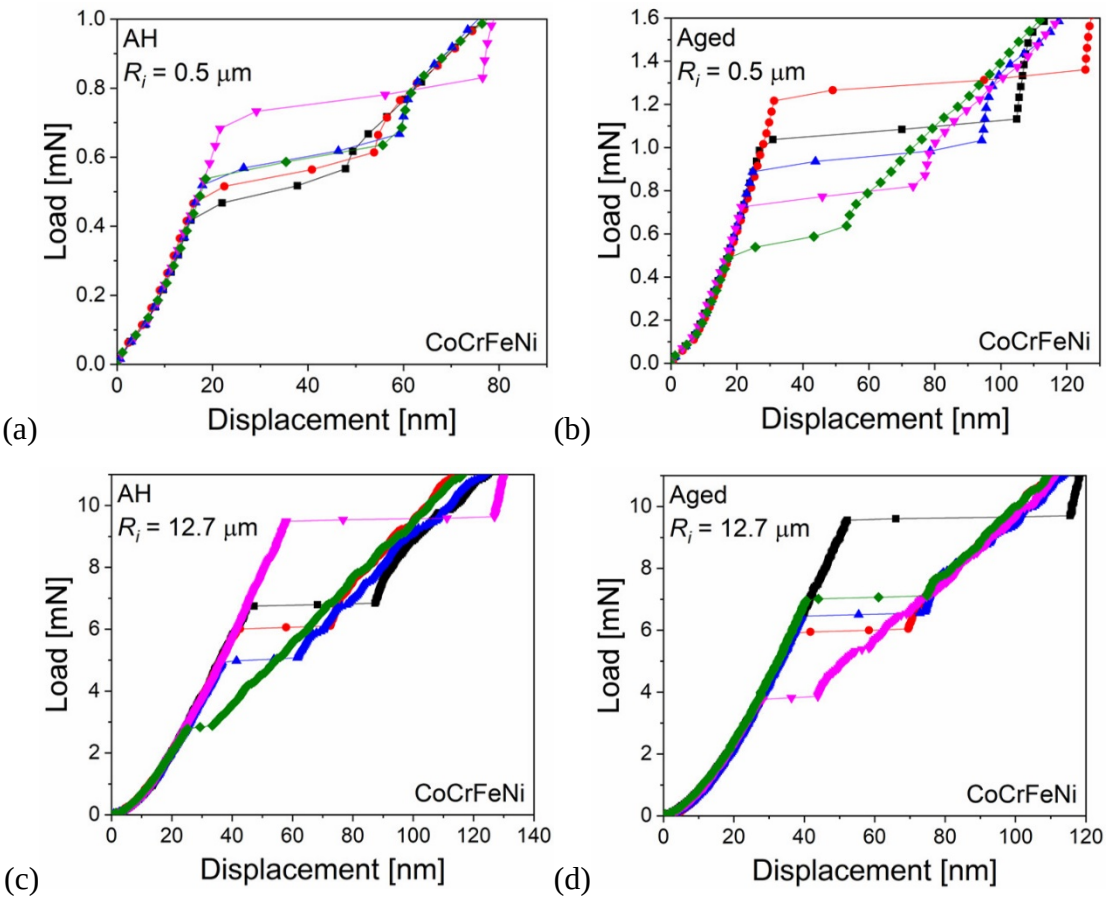

Figure S2 The representative load-displacement curves showing first pop-in in CoCrFeNi samples at R_i = 0.5 μm [(a) and (b)] and R_i = 12.7 μm [(c) and (d)]. (a) and (c) are for AH samples, while (b) and (d) are for Aged samples.

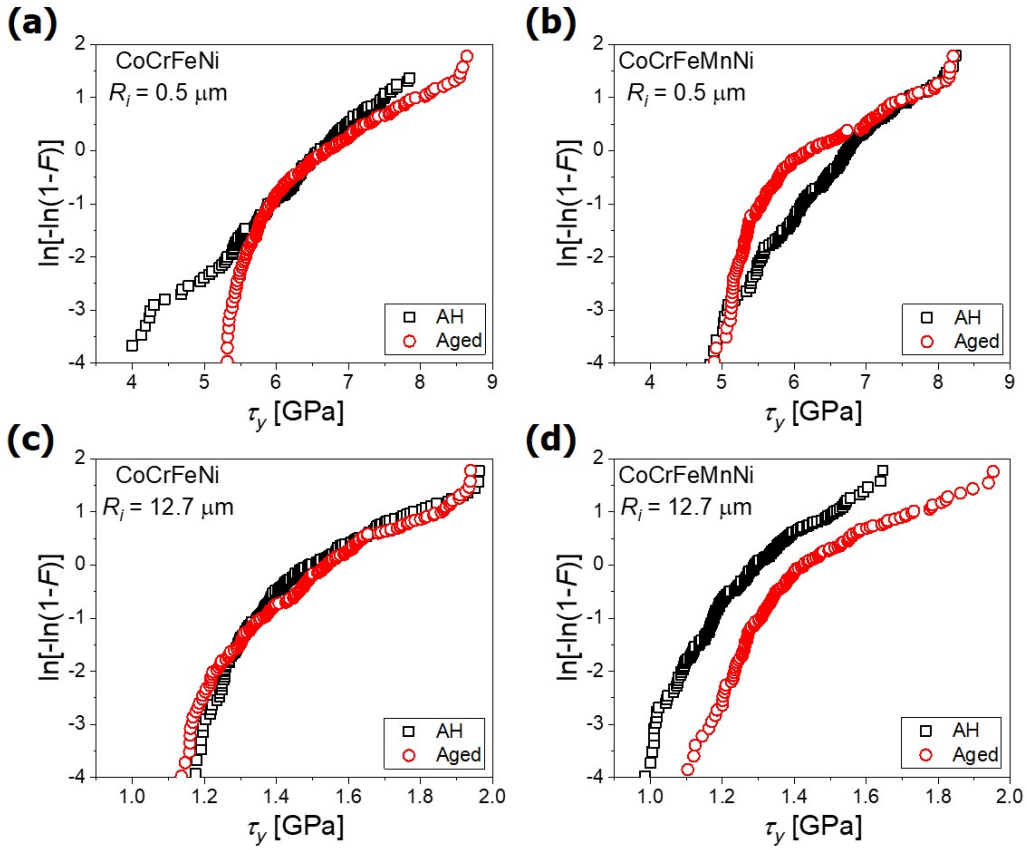

Figure S3 The plots of ln[−ln(1− F)] vs. τ_{max} at R_i = 0.5 μm [(a) and (b)] and R_i = 12.7 μm [(c) and (d)]. (a) and (c) are for CoCrFeNi, while (b) and (d) are for CoCrFeMnNi. Nearly all the curves show a non-linear feature.

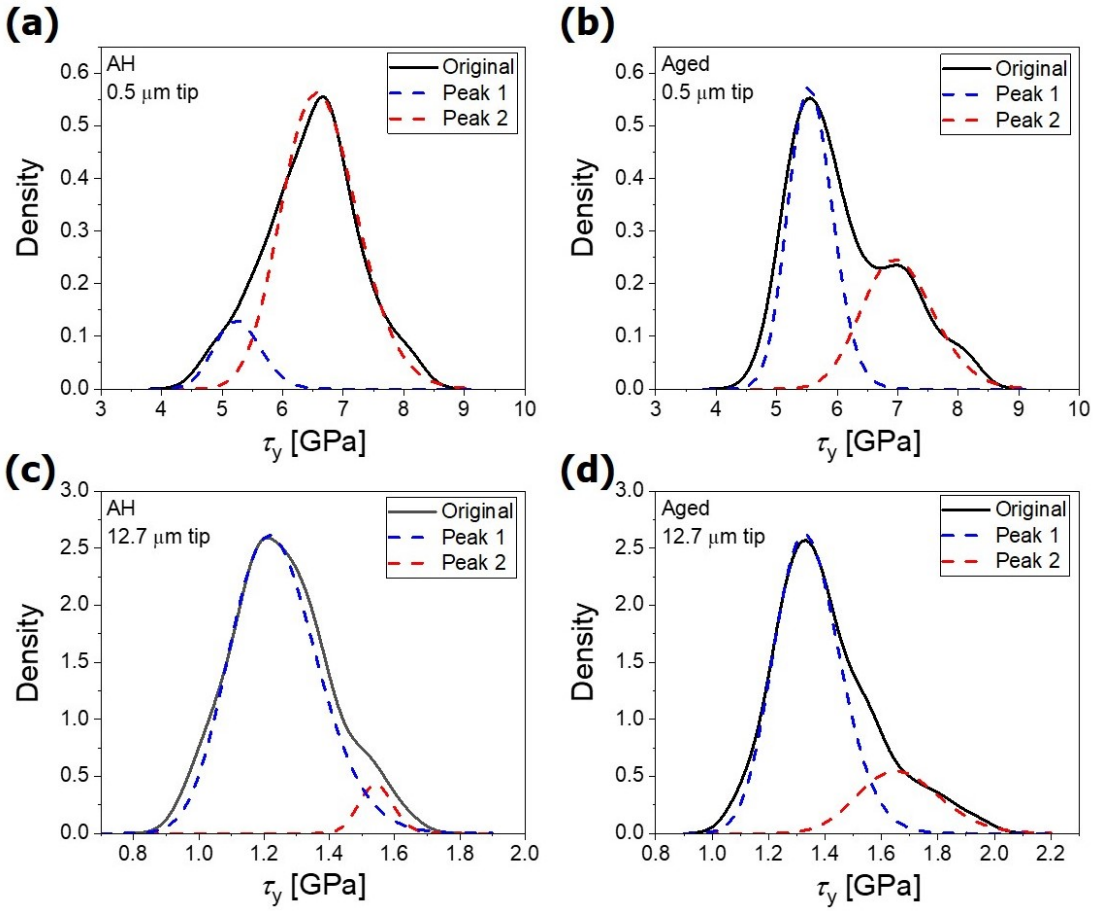

Figure S4 The examples of deconvolution results by log-normal distribution in CoCrFeMnNi samples at R_i = 0.5 μm [(a) and (b)] and R_i = 12.7 μm [(c) and (d)]. (a) and (c) are for AH samples, while (b) and (d) are for Aged samples.

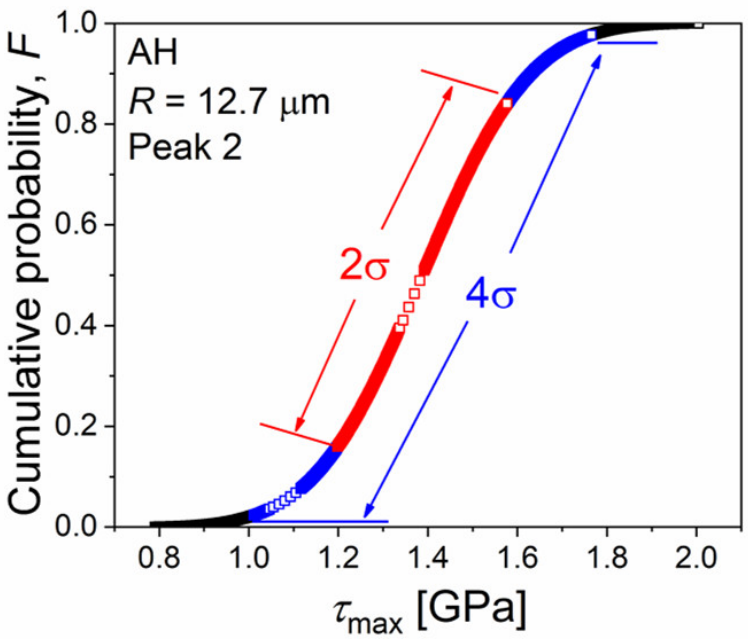

(a)

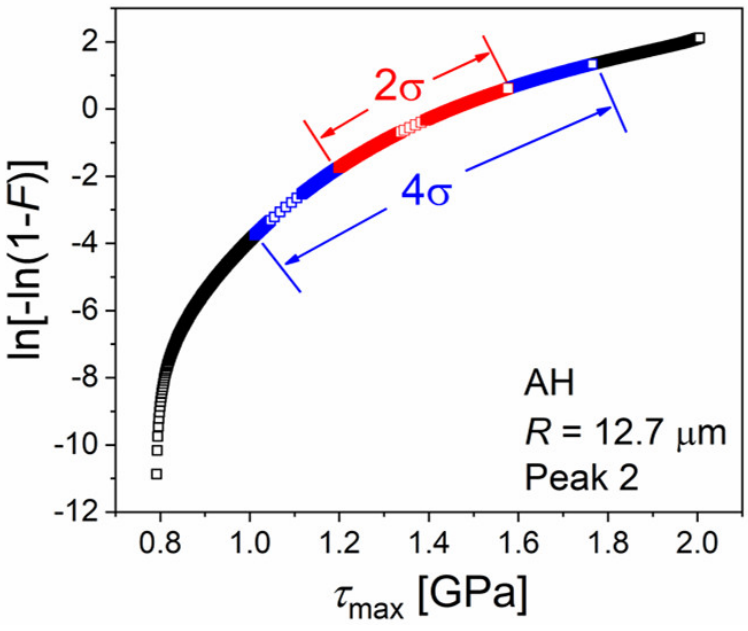

(b)

Figure S5 Examples taken to show how to cut off the tails of ln[−ln(1− F)] vs. τ_{max} plot (the deconvoluted peak 2 of AH CoCrFeMnNi sample for R_i = 12.7 μm). In Fig. S4(a), the ln[−ln(1− F)] vs. τ_{max} relation of deconvoluted peak follows a Gaussian distribution. Obviously it is not linear. But by closely comparing the curve in Fig. S4(a) with the cumulative distribution in Fig. S4(b), we found that the upper and lower tails only occupy very small fractions (in Fig. S4(a)) yet dictate the curvature shape in Fig. S4(b).

Note that most prior studies applying the same method for estimating activation volume also used only the data where ln[-ln(1-F)] value falls in the range between -2 and 1 (e.g. see Refs. [1–4]).

To cut off the tails, here we modified the "six sigma" or "6σ" (σ: standard deviation) method that is widely used in engineering as a data-driven process improvement. The application of 6σ in Gaussian distribution relies on the specific characteristics of it: About 68% of values drawn from a Gaussian distribution are within one σ away from the mean value, μ; about 95% of the values lie within two σ; and about 99.7% are within three σ. Here we revised it and used a "2σ rule" such that only the data between $\mu-\sigma$ and $\mu+\sigma$ are considered whereas the rest of the data were abandoned. In Fig. S4, it can be seen that ~68% of the data based on the "2σ rule" can well represents the major trend of the data and also results in the ln[-ln(1-F)] values falling in between -2 and 1. Therefore, our methodology can be considered reasonable and was applied in the paper.

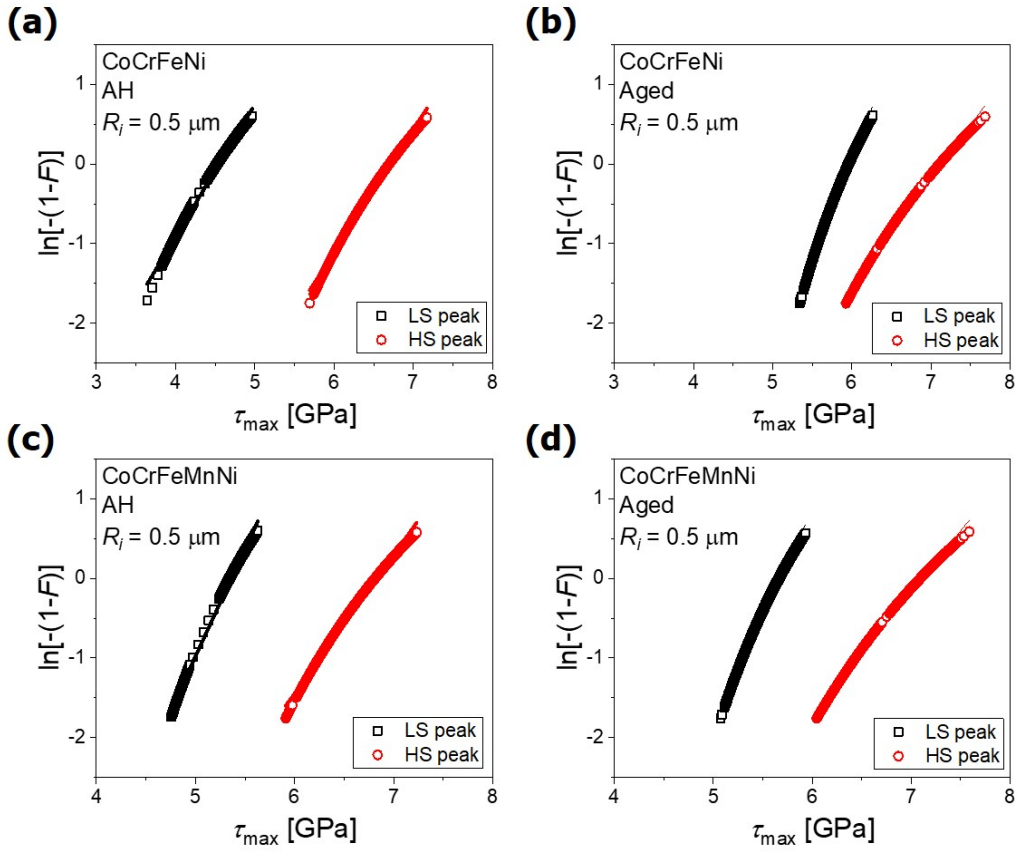

Figure S6 The examples of the plots of ln[−ln(1− F)] vs. τ_{max} relation for for R_i = 0.5 μm in CoCrFeNi [(a) and (b)] and CoCrFeMnNi samples [(c) and (d)]. (a) and (c) are for AH samples, while (b) and (d) are for Aged samples.

Maximum likelihood estimation (MLE)

If ψ and λ are subspaces of θ, such that, $\psi \cup \lambda = \theta$, the profile likelihood of ψ, $L_p(\psi)$, is defined from the following. (i) Two functions $L_\psi(\lambda) = L(\lambda|\psi)$ and $L_\lambda(\psi) = L(\psi|\lambda)$, are defined as the likelihood functions, where one parameter is held fixed while the other is varied. (ii) $\hat{\lambda}_\psi$ is defined as the value of λ at which the function $L_\psi(\lambda)$ attains a global maximum, i.e., $\hat{\lambda}_\psi = argmax_\lambda L_\psi(\lambda)$. Then, the profile likelihood $L_p(\psi)$ is $L_{\hat{\lambda}_\psi}(\psi)$. From this, $\hat{\theta}$ is deduced as follows. Let $\hat{\psi}$ be the parameter ψ for which the profile likelihood $L_p(\psi)$ attains a global maximum. Then $\hat{\theta} = \hat{\psi} \cup \hat{\lambda}_{\hat{\psi}}$.

For normal (Gaussian) and log-normal distributions, the probability density functions (PDFs), *f*(*x*), are given as:

$$f(x) = \frac{1}{\sigma\sqrt{2\pi}} \exp\left(-\frac{(x-\mu)^2}{2\sigma^2}\right) \quad \text{(S1)}$$

$$f\ (x) = \frac{1}{x\sigma\sqrt{2\pi}} \exp\left(-\frac{(ln\,x-\mu)^2}{2\sigma^2}\right), \quad x > 0 \quad \text{(S2)}$$

where μ and σ are mean and standard deviation. The closed form solutions of MLEs for Gaussian and Lognormal distributions are as follows.

(1) MLE for normal distribution:

$$\hat{\mu} = \frac{1}{n}\sum_{i=1}^{n} d_i \ , \qquad \hat{S}^2 = \frac{1}{n}\sum_{i=1}^{n}\left(d_i - \hat{S}\right)^2 \quad \text{(S3)}$$

(2) MLE for log-normal distribution:

$$\hat{\mu} = \frac{1}{n}\sum_{i=1}^{n} \ln d_i, \qquad \hat{S}^2 = \frac{1}{n}\sum_{i=1}^{n}\left(\ln d_i - \hat{S}\right)^2, \quad \text{(S4)}$$

in which *n* is the sample size.

References

[1] G. Yang, Y. Zhao, D.-H. Lee, J.-M. Park, M.-Y. Seok, J.-Y. Suh, U. Ramamurty, J. Jang, Influence of hydrogen on incipient plasticity in CoCrFeMnNi high-entropy alloy, Scr. Mater. 161 (2019) 23–27. doi:10.1016/j.scriptamat.2018.10.010.

[2] Y. Zhao, I.C. Choi, M.Y. Seok, M.H. Kim, D.H. Kim, U. Ramamurty, J.Y. Suh, J. Il Jang, Effect of hydrogen on the yielding behavior and shear transformation zone volume in metallic glass ribbons, Acta Mater. 78 (2014) 213–221. doi:10.1016/j.actamat.2014.06.046.

[3] I.C. Choi, Y. Zhao, Y.J. Kim, B.G. Yoo, J.Y. Suh, U. Ramamurty, J. Il Jang, Indentation size effect and shear transformation zone size in a bulk metallic glass in two different structural states, Acta Mater. 60 (2012) 6862–6868. doi:10.1016/j.actamat.2012.08.061.

[4] C.A. Schuh, A.C. Lund, Application of nucleation theory to the rate dependence of incipient plasticity during nanoindentation, J. Mater. Res. 19 (2004) 2152–2158. doi:10.1557/JMR.2004.0276.